Thermocapillary Flow Around Hemispherical Bubble

BERT K. LARKIN

Lomita, California

A hemispherical bubble, attached to a plate, is surrounded by an initially quiescent and isothermal liquid. By suddenly heating the plate, a thermal gradient over the bubble surface results. Because surface tension is temperature dependent, tangential stresses arise at the bubble surface. The liquid is viscous, and motion in the liquid phase begins. Such motion is an example of thermocapillary flow. This problem, besides being of interest from a fundamental point of view, is of possible concern in the design of space vehicles capable of storing cryogenic fluids for long periods of time in a weightless condition.

Solutions to the problem are developed by numerical treatment of the governing equations. Flow and temperature fields, which depend upon the Prandtl and Marangoni numbers, were obtained for Prandtl numbers 1 and 5 and Marangoni numbers from 0 to 100,000.

Results show that liquid is pulled toward the intersection of the bubble and the plate, then flows around the bubble surface, and leaves the bubble as a jet. The extent of the jet increases with increasing Marangoni number and decreases with increasing Prandtl number.

Thermocapillary flow increases heat transfer (Nusselt number) over that obtained from conduction, but the increase is modest. The Nusselt number increases with the Marangoni number and is insensitive to the Prandtl number. At a Marangoni number of 40,000, the local Nusselt number was increased by a factor of 2. In order for thermocapillary flow to become a dominant heat transfer mechanism, the Marangoni number must exceed 100,000.

Thermocapillary flow results from temperature gradients in a liquid-vapor interface. Since it is generally true that interfacial tension changes as temperature changes, thermal gradients in an interface generate tangential stresses. These stresses, in turn, induce fluid motion. Such flow is sometimes called the *Marangoni effect*. A common example of flow induced by surface tension is that in which cellular patterns develop in the drying of paint films. This latter problem has been studied rather extensively (*1* to *4*).

The storage of cryogenic fluids plays an important role in the design of space vehicles which are intended for long-term missions. Rates of heat transfer and the configuration of vapor-liquid interfaces certainly will be dependent upon the flow field within the stored fluid. Because the stored cryogenic fluids will be in an essentially weightless environment for long periods of time, flow mechanisms which may be of little importance here on Earth could become significant in space applications. Such may be the case for thermocapillary flow.

That thermocapillary flow might be of some importance as a heat transfer mechanism has been suggested by McGrew (*5, 6*) and Rohsenow (*7*). Figure 1 presents an example of thermocapillary flow. This figure is a photograph of a diode which is supported by thin wires, immersed in methanol, and heated by an electric current. On the top of the diode is a vapor bubble. From this bubble a jet of liquid emerges, and, because the axis of the jet is not vertical, it is obvious that some force other than gravity must be important in sustaining the jet. Behar (*8*) presents a photograph of thermocapillary jets. In this case several air bubbles are attached to a vertical platinum ribbon immersed in water. The thermocapillary jets make a 45 deg. angle with the ribbon.

Contradictions are not unusual in problems related to heat transfer, and the case of the importance of thermocapillary flow is no exception. Behar (*8*) studied both free and forced convection to liquids containing dissolved gases and found that dissolved gases inhibited heat transfer rates. On this basis one would conclude that thermocapillary flow does not contribute significantly to heat transfer. (In Behar's experiment, heating causes the dissolved gases to form bubbles at the heated surface, and thermocapillary jets from the bubbles could increase heat transfer.) On the other hand, McGrew (*6*), from a series of experiments, concluded that thermocapillary flow was an important heat transfer mechanism. One of the reasons for the contradiction might be contamination of test liquids with small amounts of impurities. It is well known that interfacial tensions may be greatly changed by only minute quantities of certain impurities. As will be shown later, a quantity of considerable importance to thermocapillary flow is the rate of change of interfacial tension with temperature. This quantity could also be changed by contamination. Young (*9*) noted some erratic behavior in his experiment in thermocapillary flow, and the trouble was attributed to contamination of the test fluid. To prove that contamination was the cause, Young (*9*) introduced small amounts of silicone oil into hexadecane and observed that thermocapillary flow was retarded. One of the reasons behind McGrew's conclusion that thermocapillary flow is important in nucleate boiling is that heat transfer coefficients for upward and downward facing surfaces do not

differ greatly. However, conduction heat transfer would occur regardless of surface orientation, and McGrew's experiments could not distinguish between heat flow by conduction and by thermocapillary convection.

The work presented below is analytical and treats the problem of thermocapillary flow resulting from heating an isolated hemispherical bubble attached to a planar surface. The bubble, though static itself, creates a jet in the surrounding liquid. Results are to be applied to static bubbles. Examples are the bubbles of desorbed gases resulting from the gradual heating of a liquid or perhaps a bubble of inert gas in the propellant tank of a vehicle coasting in space. If the results from this study have any application to boiling heat transfer, it would be during the bubble waiting period.

To solve the problem, the momentum, continuity, and energy equations are considered. Coupling between these equations is an essential part of the problem. For example, the temperature gradient over the bubble surface determines a shear stress boundary condition which is necessary in determining the flow field. On the other hand, the flow field, from the convective terms in the energy equation, influences the temperature gradient over the bubble surface. That such problems can be solved, at least by using a digital computer, was illustrated by Wilkes (*10*) in his work on natural convection.

Although the analysis presented below has some rather limiting assumptions, it has several advantages over experimental techniques. For example, velocity distributions can be determined over the bubble surface. True weightlessness can be achieved here on Earth; hence, contributions from gravity induced convection are not present. By no means does the author intend to imply that the problem can be solved solely by analytical methods. Data such as bubble diameter and nucleation site density must be obtained from experiments. However, it is believed that the results provide a greater understanding of the problem and may be helpful in the design of experiments.

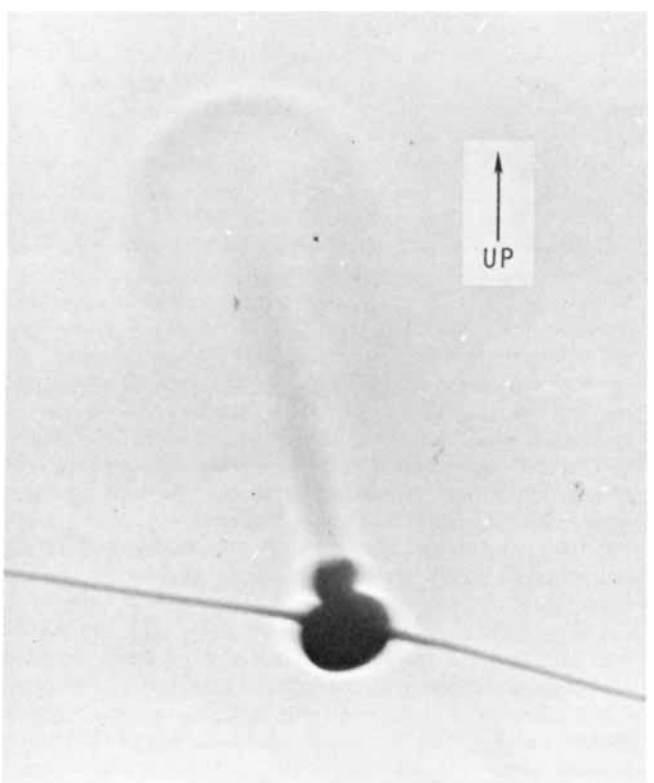

Fig. 1. A thermocapillary jet.

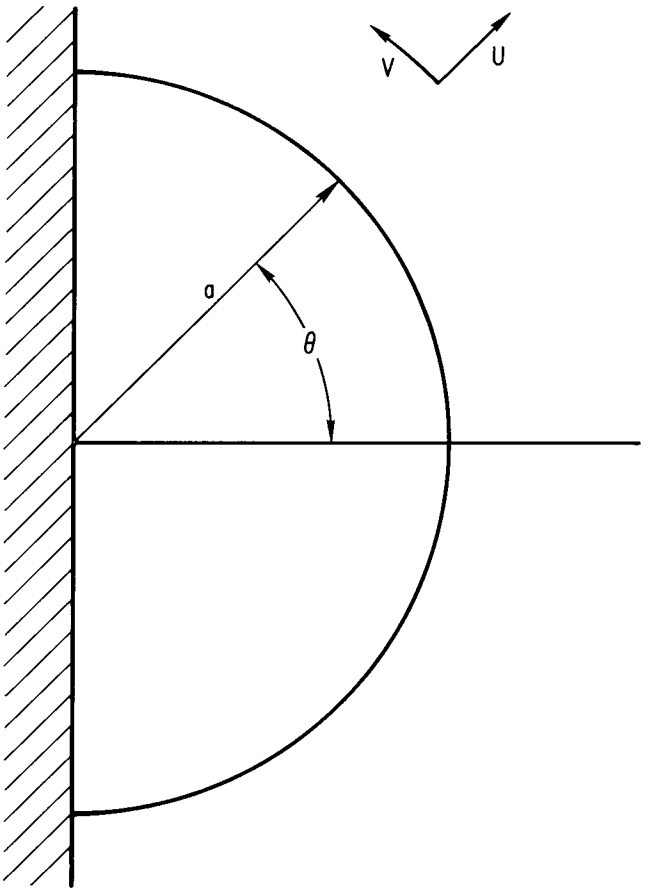

Fig. 2. Bubble schematic.

MATHEMATICAL FORMULATION

Consider a single bubble (a hemisphere), Figure 2, attached to a planar surface and surrounded in liquid. Initially, the temperature is uniform, and the fluids are motionless. At time zero, heat is produced within the solid material comprising the wall at a uniform volumetric rate. Because of the Marangoni effect, motion of liquid begins.

Assumptions utilized in the analysis are as follows:

1. Motion is two dimensional.
2. The liquid is incompressible.
3. Gas conductivity is zero, but liquid conductivity is finite.
4. Gas viscosity is zero, but liquid viscosity is finite.
5. Kinetic energy and dissipation terms in energy equation are negligible.
6. There are constant physical properties.
7. The heat flux distribution can be approximated by a uniform flux through the part of the surface wetted by liquid and can be assumed zero under the bubble.

The energy, continuity, and momentum equations are

$$\rho c\left(\frac{\partial T}{\partial t}+u\frac{\partial T}{\partial r}+\frac{v}{r}\frac{\partial T}{\partial \theta}\right)=\frac{k}{r^2}\left[\frac{\partial}{\partial r}\left(r^2\frac{\partial T}{\partial r}\right)+\frac{1}{\sin\theta}\frac{\partial}{\partial \theta}\left(\sin\theta\frac{\partial T}{\partial \theta}\right)\right] \quad (1)$$

$$\frac{1}{r}\frac{\partial}{\partial r}(r^2u)+\frac{1}{\sin\theta}\frac{\partial}{\partial \theta}(v\sin\theta)=0 \quad (2)$$

$$\frac{\partial u}{\partial t}+u\frac{\partial u}{\partial r}+\frac{v}{r}\frac{\partial u}{\partial \theta}-\frac{v^2}{r}=\frac{-1}{\rho}\frac{\partial P}{\partial r}+\nu\left(\nabla^2u-\frac{2u}{r^2}-\frac{2}{r^2}\frac{\partial v}{\partial \theta}-\frac{2v}{r^2}\cot\theta\right) \quad (3)$$

$$\frac{\partial v}{\partial t} + u\frac{\partial v}{\partial r} + \frac{v}{r}\frac{\partial v}{\partial \theta} + \frac{uv}{r} = \frac{-1}{\rho r}\frac{\partial P}{\partial \theta} + \nu\left(\nabla^2 v + \frac{2}{r^2}\frac{\partial u}{\partial \theta} - \frac{v}{r^2 \sin^2\theta}\right) \quad (4)$$

Initial conditions are

$$u(r,\theta) = v(r,\theta) = 0, \quad T(r,\theta) = T_0 \quad (5)$$

Boundary conditions are:

on $\theta = \pi/2, \quad r > a, \quad t > 0$

$$u = v = 0, \quad \frac{k}{r}\frac{\partial T}{\partial \theta} = q \quad (6)$$

on $\theta = 0, \quad r > a, \quad t > 0$

$$\frac{\partial T}{\partial \theta} = \frac{\partial u}{\partial \theta} = 0, \quad v = 0 \quad (7)$$

$\lim r \to \infty, \quad 0 < \theta < \pi/2, \quad t > 0$

$$u = v = 0, \quad T = T_0 \quad (8)$$

on $r = a, \quad 0 < \theta < \pi/2, \quad t > 0$

$$\frac{\partial T}{\partial r} = u = 0, \quad \frac{-\beta}{a}\frac{\partial T}{\partial \theta} = \rho\nu\left(\frac{\partial v}{\partial r} - \frac{v}{a}\right) \quad (9)$$

Of the above boundary conditions, only those applied at the bubble surface should require any explanation. There is no flow normal to the surface; hence, u is zero. Because the gas in the bubble is assumed to have a negligible conductivity, the radial temperature gradient (in the liquid) must be zero. The assumption of zero gas conductivity is a convenient mathematical abstraction and is based upon the fact that conductivities of gases are generally much smaller than those of liquids. Additional support for this assumption comes from explanations of the mechanism of nucleate boiling. Rohsenow (7) states that only a very small part of the heat transferred from the heating surface is directly transferred to the interior of bubbles adhering to the surface. The main part of the energy is transferred directly to the liquid. Unlike most problems concerning flow at solid boundaries, the tangential velocity component v is not zero at the interface. A balance in tangential stresses (those of viscous shear and interfacial tension) leads to the latter portion of Equation (9). This particular equation may be derived from the work of Young (9) by using the assumption of negligible viscosity of gas inside the bubble. It is this boundary condition which allows thermocapillary flow by its coupling of the energy and momentum equations.

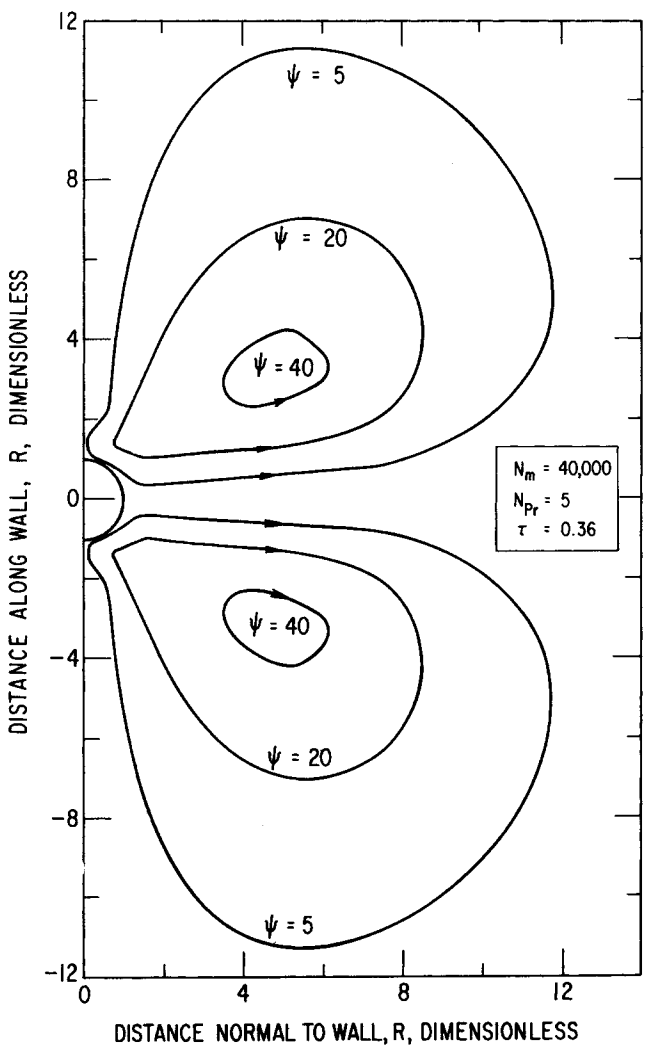

Fig. 3. Typical streamlines.

As a means of simplifying the solution of the problem, dimensionless variables are introduced, and, by means of these new variables, the governing equations become

$$\frac{\partial T'}{\partial \tau} + U\frac{\partial T'}{\partial R} + \frac{V}{R}\frac{\partial T'}{\partial \theta} = \frac{1}{R^2}\left[\frac{\partial}{\partial R}\left(R^2\frac{\partial T'}{\partial R}\right) + \frac{1}{\sin\theta}\frac{\partial}{\partial \theta}\left(\sin\theta\frac{\partial T'}{\partial \theta}\right)\right] \quad (10)$$

$$\frac{1}{R}\frac{\partial}{\partial R}(R^2 U) + \frac{1}{\sin\theta}\frac{\partial}{\partial \theta}(V\sin\theta) = 0 \quad (11)$$

$$\frac{\partial U}{\partial \tau} + U\frac{\partial U}{\partial R} + \frac{V}{R}\frac{\partial U}{\partial \theta} - \frac{V^2}{R} = -\frac{a^2}{\rho\alpha^2}\frac{\partial P}{\partial R} + N_{Pr}\left[\nabla^2 U - \frac{2U}{R^2} - \frac{2}{R^2}\frac{\partial V}{\partial \theta} - \frac{2V\cot\theta}{R^2}\right] \quad (12)$$

$$\frac{\partial V}{\partial \tau} + U\frac{\partial V}{\partial R} + \frac{V}{R}\frac{\partial V}{\partial \theta} + \frac{UV}{R} = -\frac{a^2}{\rho\alpha^2 R}\frac{\partial P}{\partial \theta} + N_{Pr}\left[\nabla^2 V + \frac{2}{R^2}\frac{\partial U}{\partial \theta} - \frac{V}{R^2\sin^2\theta}\right] \quad (13)$$

Initial and boundary conditions, Equations (5) through (9), are readily obtained for the dimensionless variables and will not be repeated. An important dimensionless group, the Marangoni number, is generated in the stress balance portion of Equation (9):

on $R = 1, \quad 0 < \theta < \pi/2, \quad \tau > 0$

$$\frac{\partial V}{\partial R} - V = N_M\frac{\partial T}{\partial \theta} \quad (14)$$

According to Pearson (1), the Marangoni number expresses the relative importance of surface tension forces and viscous forces.

Of possible benefit in the design of experiments in thermocapillary flow is the fact that only two dimensionless groups appear in the governing equation, the Prandtl and Marangoni numbers.

COMPUTATIONAL TECHNIQUES

Problems of this type have been solved numerically by several authors (10 to 12), and, in the interest of saving space, only a sketch of the tedious process of solving the equations will be presented. Persons interested in numerical details may secure a copy of the Fortran program by requesting one from the author.

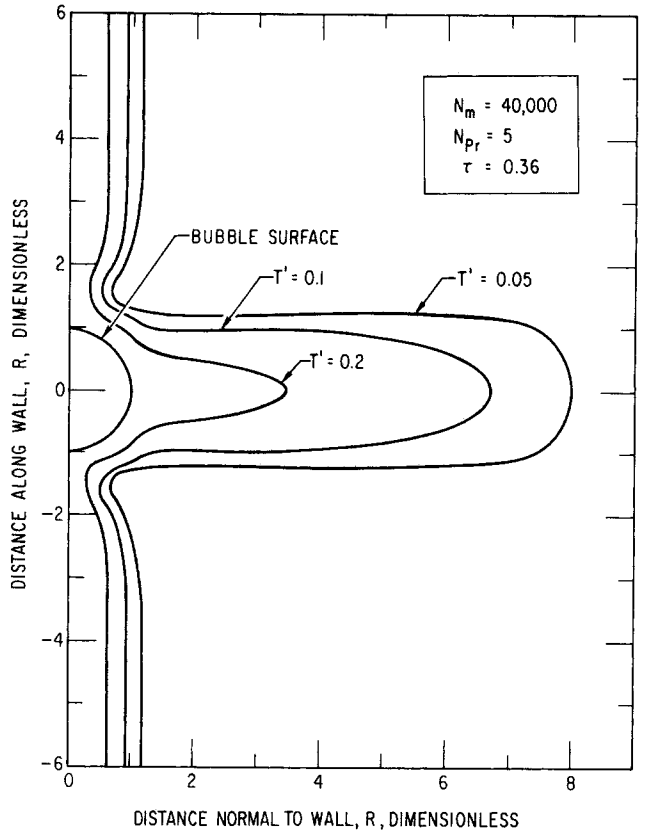

Fig. 4. Typical isotherms.

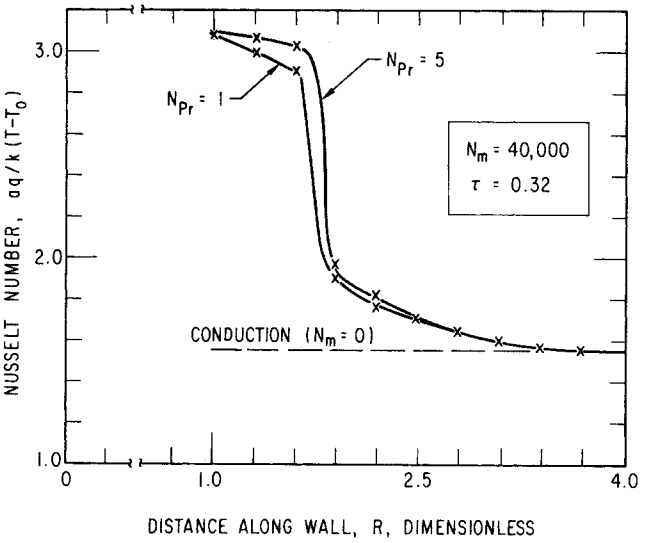

Fig. 5. Local Nusselt number.

A stream function ψ and a vorticity S^* are introduced as new dependent variables, replacing U, V, and P. By using the stream function to define the velocity components

$$U = \frac{1}{R^2 \sin\theta}\frac{\partial\psi}{\partial\theta}, \quad V = \frac{-1}{R\sin\theta}\frac{\partial\psi}{\partial R} \tag{15}$$

the continuity equation is automatically satisfied.

Pressure terms are eliminated between Equations (12) and (13). This is effected by multiplying Equation (13) by R and then differentiating with respect to R. Next, Equation (12) is differentiated with respect to θ. Upon subtraction of the two momentum equations, the pressure terms vanish, and the resulting equation is

$$\frac{\partial S}{\partial\tau} + \frac{\partial(US)}{\partial R} + \frac{1}{R}\frac{\partial(VS)}{\partial\theta} = N_{Pr}\left[\frac{\partial^2 S}{\partial R^2} + \frac{1}{R^2}\frac{\partial^2 S}{\partial\theta^2} - \frac{S}{R^2\sin^2\theta} + \frac{\cot\theta}{R^2}\frac{\partial S}{\partial\theta}\right] \tag{16}$$

The elliptic equation relating S to the stream function is

$$-S\sin\theta = \frac{\partial^2\psi}{\partial R^2} + \frac{1}{R^2}\frac{\partial^2\psi}{\partial\theta^2} - \frac{\cot\theta}{R^2}\frac{\partial\psi}{\partial\theta} \tag{17}$$

Numerical solution of the problem requires solving Equations (10), (16), and (17). Over each time step, Equation (10) was solved by an alternating direction implicit method (*13*); then Equation (16) was solved by the Dufort-Frankel method (*14*), and finally Equation (17) was solved by successive overrelaxation (*15*).

Certain factors combine to make this a difficult problem even for a computer such as the CDC-6600 on which the program was run. The boundary condition at infinity, Equation (8), was approximated at $R = 16$. By trial calculation, this was found to be sufficiently large so that the thermocapillary jet was not dissipated by the artificial boundary. To provide information on the flow field around the bubble, a value of ΔR of 0.3 was found to be suitable. Hence, fifty-one grid points in the radial direction were used.

Approximating the heat flux boundary condition, Equation (6), with accuracy requires $\Delta\theta$ to be small. When fluid velocities are low, the heat flow problem closely approximates the well-known case of constant heat flow into an infinite slab, see p. 131 of Churchill (*16*). To compute wall temperatures to an accuracy of within 3% of the analytical solution at zero Marangoni number (no fluid flow), it was necessary to use twenty-five grid points in the theta direction. Hence, 1,275 grid points were used in generating the numerical solutions.

Instabilities, apparently caused by the nonlinear convective terms in Equations (10) and (16) were noted at high flows. This made it necessary to employ smaller time steps as the Marangoni number increased. At N_M = 100,000, it was necessary to use $\Delta\tau = 0.0008$. The combination of many grid points and small time step required considerable time on the computer. A typical run required ½ hr.

ILLUSTRATIVE RESULTS

Because this problem taxes the capacity of even a large computer, the number of solutions which were developed is not large. However, the results do show in quantitative form the resulting flow fields and help define conditions under which thermocapillary flow becomes an important heat transfer mechanism.

All flow fields were found similar to the one illustrated in Figure 3. Since the lines of constant stream function are tangent to the velocity field, they indicate the direction of flow. Arrows show the direction of circulation. Circulation is observed both above and below the bubble. Because of the interfacial shear stress, liquid is pulled toward the wall, then flows around the hemispherical interface, and finally converges into a jet which flows outward from the wall. Significant flows near the wall were noted only in the vicinity of the bubble.

Figure 4 illustrates the isotherms which are characteristic of this problem. In the region near the wall, yet far from the bubble, the isotherms tend to form parallel vertical lines. Here the flow is very small, and in this region isotherms are characteristic of those for conductive heat

* The vorticity is the curl of the velocity and has but one component in this problem. Strictly speaking, S is not the vorticity but is R times the vorticity. For lack of a better term, S is called the vorticity.

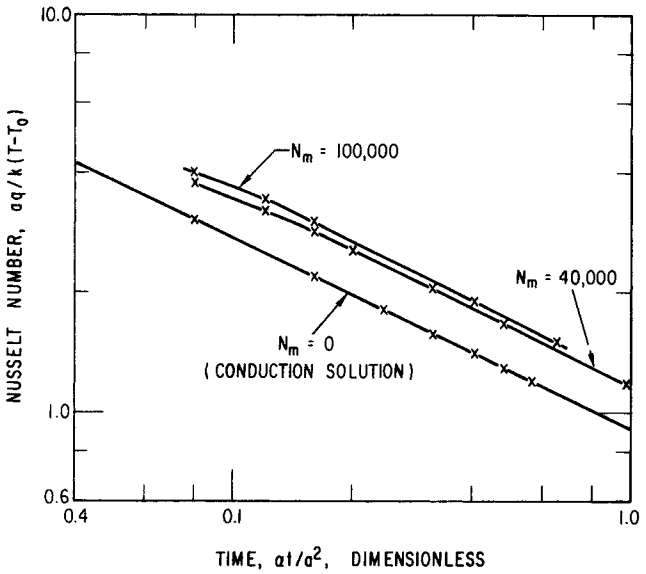

Fig. 6. Average Nusselt number.

flow into a semi-infinite slab. Bending of the isotherms toward the wall is noted in the region near the bubble. This bending results from the flow of cool liquid toward the wall as shown on Figure 3. The liquid jet, in flowing outward from the wall, causes the isotherms to project outward. From Figure 4, it is obvious that the thermocapillary flow field is increasing heat transfer, at least in the region near the bubble.

The Nusselt number, based upon bubble radius, is simply the reciprocal of the dimensionless wall temperature. Plotted in Figure 5 is the local Nusselt number for the conditions indicated on the figure. Near the bubble the Nusselt number is relatively high, while a sharp decrease is observed at about 1.8 radii. At large radii the curve approaches the limiting value for the conduction solution. Qualitatively, this behavior is to be inferred from Figures 3 and 4. Figure 4 shows bending of the isotherms toward the wall only near the bubble, while Figure 3 shows the streamlines tending to converge near the line of contact between the bubble and the wall. Note that the curves for Prandtl numbers 1 and 5 do not differ significantly. This similarity was observed in all runs.

Whether or not thermocapillary flow is an important heat transfer mechanism requires making a number of assumptions. For example, in finding an average Nusselt number from data presented in Figure 5, it is necessary to limit the extent of integration. This follows from the assumption of a single bubble surrounded by an infinite amount of liquid. Integration of the data of Figure 5 over an infinite radius leads to the obvious result that thermocapillary flow does not influence the average Nusselt number. Of more practical interest is the case of many bubbles attached to a wall. Based upon the entirely arbitrary assumption that bubbles are located 6 radii apart, the average Nusselt number is approximated by integrating the local values for a single bubble over 3 radii. On this basis, Figure 6 was prepared and shows average Nusselt number vs. time for values of the Marangoni number up to 100,000. The intent is merely to provide the reader with a feeling for the order of magnitude of the effect of thermocapillary flow on heat transfer. In every case the Nusselt number was observed to decrease with time, and the impact of thermocapillary flow on heat transfer was not great. Only a 30% increase in heat transfer was realized at a Marangoni number of 100,000. From the figure it is evident that a Marangoni number in excess of 100,000 is necessary in order that thermocapillary flow be an important heat transfer mechanism.

Calculations of average Nusselt numbers were found to be insensitive to Prandtl numbers. Prandtl numbers of 1 and 5 gave virtually identical Nusselt numbers. However, Nusselt numbers did vary with time and Marangoni numbers, as Figure 6 shows. Except for very early times, the lines of Figure 6 are essentially parallel and have a slope of minus one-half. At early values of time the flow fields have little influence on heat transfer, and all curves converge to that for the conduction solution.

The calculation of a Marangoni number for typical space storage of hydrogen is a speculative task. Of the parameters entering the definition of the Marangoni number, the bubble radius is the most difficult to determine. There are no long-term data, and it will be assumed, arbitrarily, that the bubble radius is 1 cm. The study of Cody and Hyde (*17*) indicates that a heat flux of 0.2 B.t.u./(hr.)(sq.ft.) is reasonable to assume for space storage of hydrogen. Liquid hydrogen properties necessary for computing the Marangoni number are

N_{Pr}	1.0
β	−0.17 dynes/(cm.)(°K.)
ρ	0.071 g./cc.
c	2.2 cal./(g.)(°K.)
α	1.74×10^{-3} sq.cm./sec.

From these data it follows that the typical Marangoni number is 44,000. Figure 6 shows that for such values of the Marangoni number, thermocapillary flow is not a heat flow mechanism of overwhelming importance. Increases in bubble radius would greatly increase the Marangoni number, since the radius squared is a factor. Hence, the importance of thermocapillary flow as a heat transfer mechanism in hydrogen requires bubble radii in excess of 1 cm.

Even though a number of assumptions were necessary in making estimates of the importance of thermocapillary

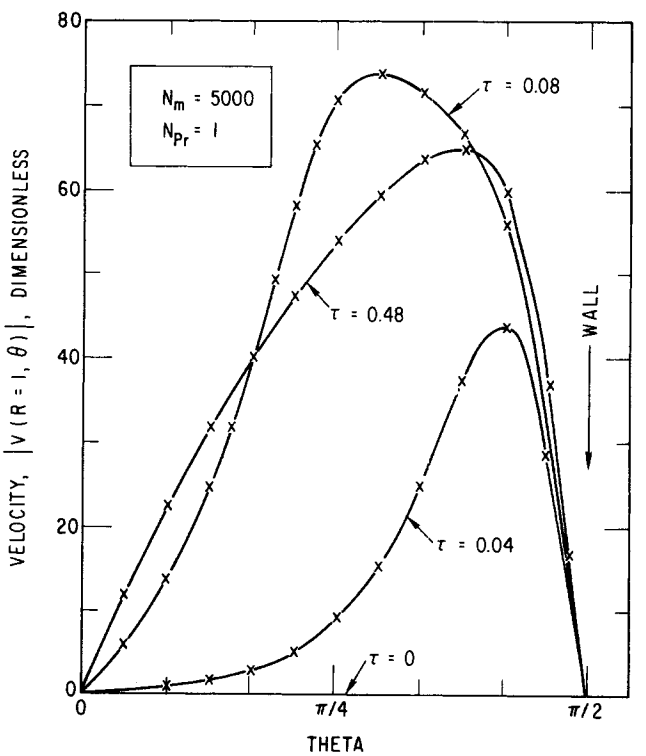

Fig. 7. Interface velocity distribution.

flow as a heat transfer mechanism, some limiting conditions do exist. From Figure 5, the local Nusselt number was increased at most by a factor of 2. Hence, in cases of extremely high bubble density, the mechanism of thermocapillary flow could increase heat transfer by 100% over that for conduction. Larger Marangoni numbers would lead to larger Nusselt numbers, of course.

It could be argued that this is a transient process, and the contribution to heat flow by conduction decreases with time. (Nusselt numbers for conduction vary as the minus one-half power of time.) Perhaps thermocapillary flow becomes more important as time increases. Numerical results, while not conclusive, are not very encouraging on this point. The longest run was to $\tau = 1.6$. For the conditions of hydrogen storage cited above, this represents a real time of about 15 min. Over the duration of the computer run there was no tendency toward a leveling off of the process. After an initial transient, fluid velocities were slowly decreasing with increasing time.

Calculations illustrative of the interface flow are given in Figure 7. For the coordinates of this problem, surface flows are negative in value, and Figure 7 shows only magnitudes of these tangential flows. At time zero, the flow is zero at all angles. At time 0.04, the flow has reached a maximum of 45 at a point near the wall. Later, at time 0.08, the velocities have increased in magnitude, and the maximum has shifted away from the wall. Still later in the time scale, at time 0.48, the velocities have decreased in magnitude, and the maximum has moved back toward the wall. These general results were observed in every run. That is, velocities increased rapidly from zero to a maximum and then decreased slowly, with increasing time. This behavior points out a certain self-regulating character about the mechanism of thermocapillary flow. High thermal gradients generate large flows which tend to erase the high thermal gradients. Negative feedback seems to be characteristic of this process.

Streaming from the bubble is a jet of liquid which is attenuated with increasing distance. This behavior is illustrated by Figure 8, a plot of radial velocity at theta equals 0 deg. Viscous forces evidently play an important role in determining the velocity distribution. As the Prandtl number decreases from 5 to 1, the maximum velocity increases, and the jet extends farther into the liquid.

Figure 9 also shows the radial velocity distribution of the jet. It is noted that maximum velocity and the extent of the jet increase with increasing Marangoni number. The fact that the jet extends so far into the liquid may be of some concern in the application of devices to position liquid-vapor interfaces in low gravity. For example, screens depend upon capillary forces to separate liquid and vapor phases. A thermocapillary jet might propel liquid through the screen, thus destroying the effectiveness of the control device.

CONCLUSIONS

From the governing equations, it was found that thermocapillary flow fields depend upon Prandtl and Marangoni numbers. Numerical solutions can be obtained for Prandtl numbers of 1 and 5 and Marangoni numbers from 0 to 100,000.

As a result of thermocapillary stress, flow fields developed from an initially quiescent liquid. Results show that liquid is pulled toward the intersection of the bubble with the wall, then it flows around the bubble surface to emerge as a jet leaving the bubble. These jets were found to extend as far as 9 radii from the wall.

Increased heat transfer was noted as a result of fluid motion. Local Nusselt numbers increased by a factor of 2 over those corresponding to the conduction solution. Average Nusselt numbers showed a smaller increase. Before

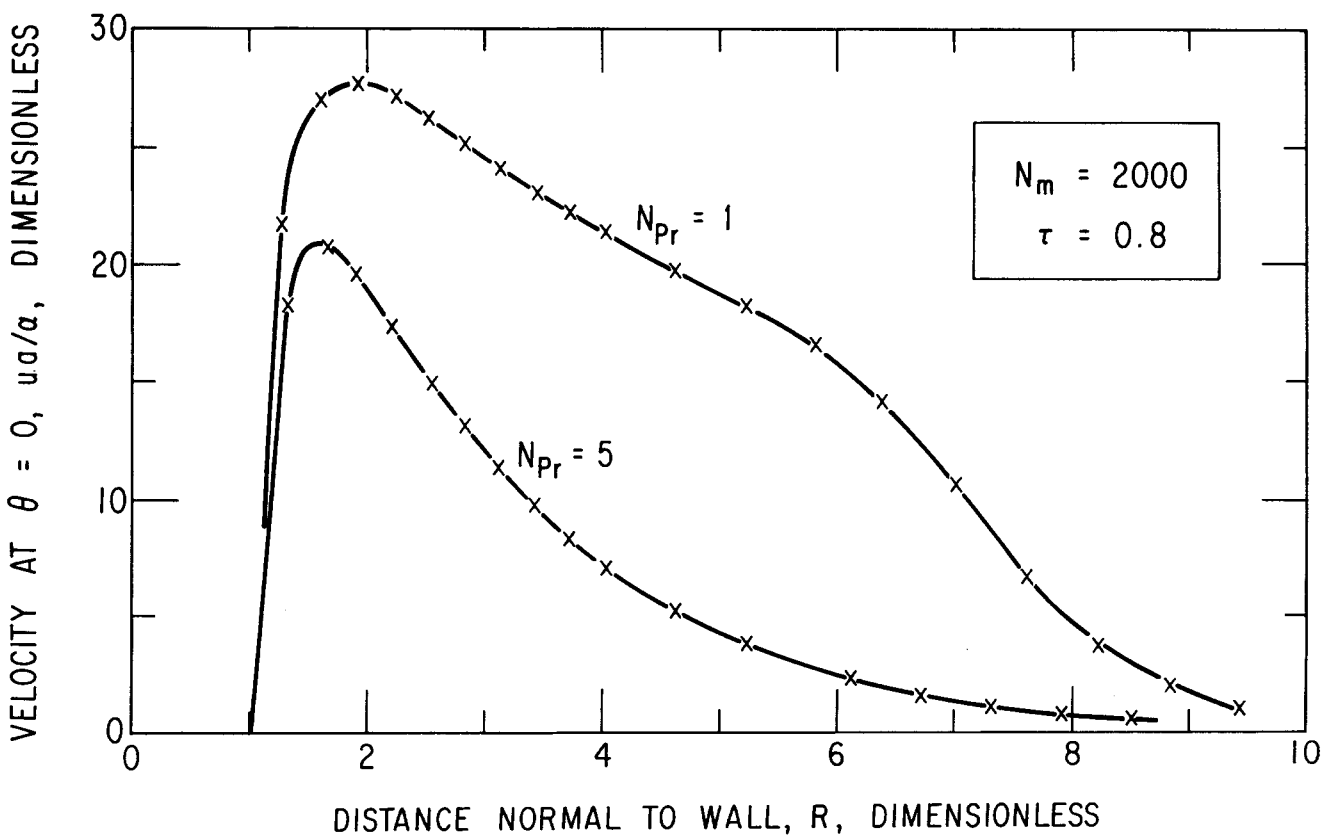

Fig. 8. Effect of Prandtl number on radial velocity.

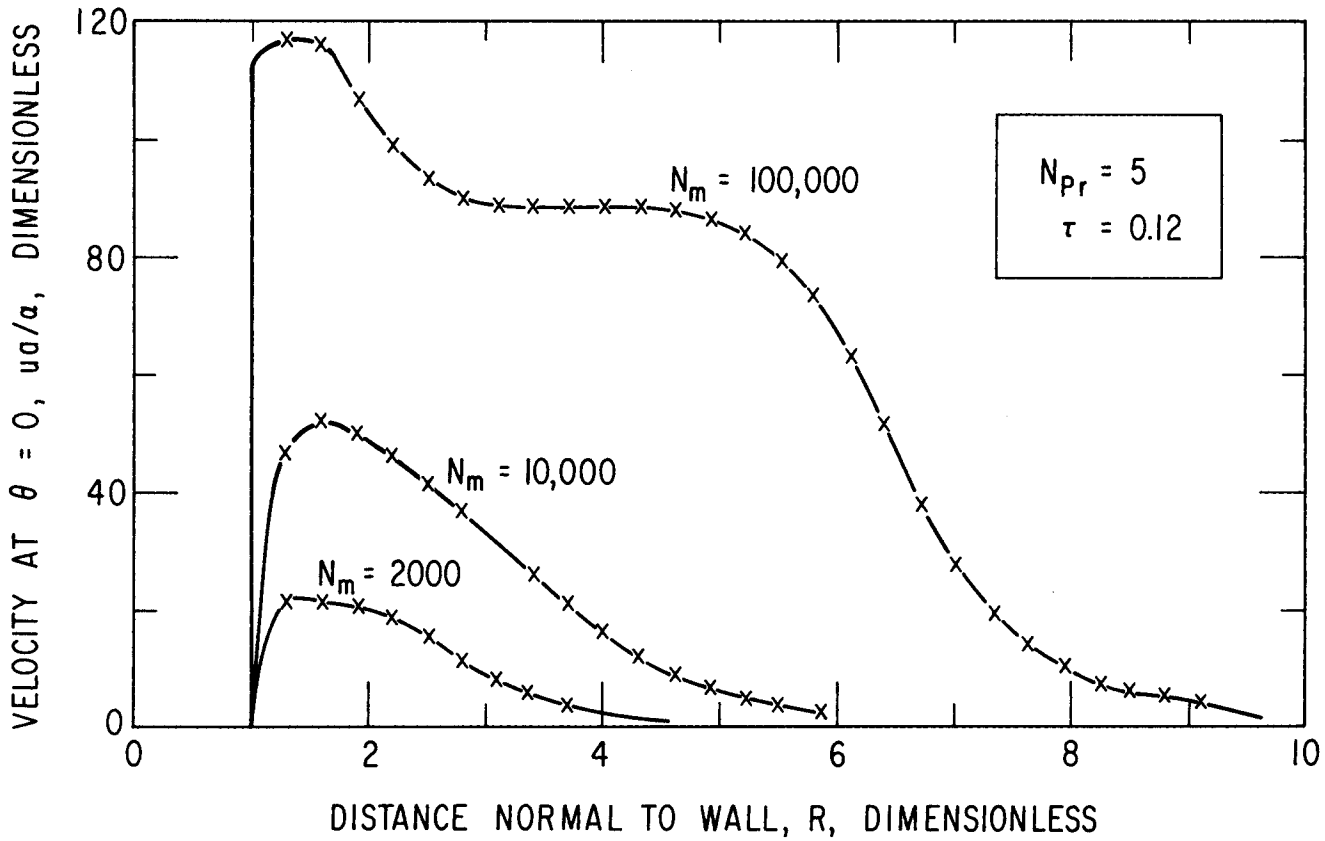

Fig. 9. Effect of Marangoni number on radial velocity.

thermocapillary flow becomes a mechanism of dominant importance, the Marangoni number must exceed 100,000.

ACKNOWLEDGMENT

The generosity of T. E. Bowman in furnishing Figure 1 is gratefully acknowledged.

NOTATION

a = bubble radius
c = specific heat
k = thermal conductivity
N_M = $-\beta q\ a^2/k\rho\nu\alpha$, Marangoni number
N_{Pr} = Prandtl number
P = pressure
q = wall heat flux
r = radius
R = r/a
S = $V + R\dfrac{\partial V}{\partial R} - \dfrac{\partial U}{\partial \theta}$
t = time
T = temperature
T_0 = initial temperature
T' = $(T - T_0)k/aq$
u = radial velocity component
U = ua/α
v = theta velocity component
V = va/α

Greek Letters

α = thermal diffusivity
β = derivative of surface tension with respect to temperature (assumed as constant)
θ = angle
ν = kinematic viscosity
ρ = density
τ = $\alpha t/a^2$
ψ = stream function

LITERATURE CITED

1. Pearson, J. R. A., *J. Fluid Mech.*, **4**, 489 (1958).
2. Sternling, C. V. and L. E. Scriven, *AIChE J.*, **5**, 514 (1959).
3. Smith, K. A., *J. Fluid Mech.*, **24**, 401 (1966).
4. Berg, J. C., M. Boudart, and A. Acrivos, *ibid.*, 721.
5. McGrew, J. L., F. L. Bamford, and T. R. Rehm, *Sci.*, **153**, 1106 (1966).
6. McGrew, J. L., F. L. Bamford, and D. Brown, paper presented at Am. Inst. Chem. Engrs. 62, National Meeting, Salt Lake City, Utah (1967).
7. Rohsenow, W. M. "Developments in Heat Transfer," Mass. Inst. Technol. Press., Cambridge (1964).
8. Behar, M., M. Courtaud, R. Ricque, and R. Semeria, *Proc. Third Internatl. Heat Transfer Conf.*, **4**, 1 (1966).
9. Young, N. O., J. S. Goldstein, and M. J. Block, *J. Fluid Mech.*, **6**, 350 (1959).
10. Wilkes, J. O., Ph.D. thesis, Univ. Mich., Ann Arbor (1965).
11. Aziz, K., and J. D. Hellums, *Phys. Fluids*, **10**, 314 (1967).
12. Barakat, H. Z., H. Merte, and J. A. Clark, "Proceedings of the Conference on Long-Term Cryo-Propellant Storage in Space," Natl. Aeronaut. Space Admin., Huntsville, Ala. (1966).
13. Peaceman, D. W., and H. H. Rachford, Jr., *J. Soc. Ind. Appl. Math.*, **3**, 28 (1955).
14. Dufort, E. C., and S. P. Frankel, *Math Tables and Other Aids to Computation*, **7**, 135 (1953).
15. Frankel, S. P., *ibid.*, **4**, 65 (1950).
16. Churchill, R. V., "Operational Mathematics," 2 ed., McGraw-Hill, New York (1958).
17. Cody, J. C., and E. H. Hyde, "Proceedings of the Conference on Long-Term Cryo-Propellant Storage in Space, Natl. Aeronaut. Space Admin., Huntsville, Ala. (1966).

Manuscript received July 9, 1968; revision received July 26, 1968; paper accepted July 29, 1968.